Electronic Supplementary Information

Endo-Functionalized Molecular Cage for Selective Potentiometric Determination of Creatinine

Yu Lu,[‡a] Song-Meng Wang,[‡b] Sui-Sui He,[‡a] Qicheng Huang,[‡b] Cheng-Da Zhao,[a,c] Shan Yu,[c] Wei Jiang,[b] Huan Yao,[*a] Li-Li Wang[*a] and Liu-Pan Yang[*a]

[a.] *School of Pharmaceutical Science, Hengyang Medical School, University of South China, Hengyang, Hunan, 421001, China; *E-mail: yaoh@usc.edu.cn; wangll@usc.edu.cn; yanglp@usc.edu.cn.*

[b.] *Department of Chemistry, Southern University of Science and Technology, Xueyuan Blvd 1088, Shenzhen, 518055, China.*

[c.] *The Affiliated Nanhua Hospital, University of South China, Hengyang, Hunan 421001, China.*

Table of Contents

1. General Methods

1.1. General. All the reagents and guest molecules involved in this research were commercially available and used without further purification unless otherwise noted. Solvents were either employed as purchased or dried prior to use by standard laboratory procedures. Thin-layer chromatography (TLC) was carried out on 0.25 mm Yantai silica gel plates (60F-254). Column chromatography was performed on silica gel 60 (Tsingdao 40 – 63 nm, 200 - 400 mesh). ^{1}H, and ^{13}C NMR spectra were recorded on a Bruker Avance-400 or 500 NMR spectrometer at 25 ^{o}C. All chemical shifts are reported in ppm with residual solvents or TMS (tetramethylsilane) as the internal standards. The following abbreviations were used to report the multiplicity for NMR resonances: s = singlet; d = doublet; dd = doublet of doublet; t = triplet, m = multiplet. The NMR spectra of several compounds were measured in CD_2Cl_2 instead of $CDCl_3$, because those compounds are easily decomposed in $CDCl_3$, presumably due to the acidic property of $CHCl_3$. Electrospray-ionization high-resolution mass spectrometry (ESI-HRMS) experiments were conducted on an applied Q EXACTIVE mass spectrometry system. Ultrapure water was purified from Chuangchun pure water machine CCH-H200. ITC Titration experiments were carried out at 25 °C on a Nano ITC LV – 190 μL (Waters GmbH, TA Instruments, Eschborn, Germany). The titration experiments were repeated three times, and the averaged values and standard deviations were given. The urine and plasma samples were collected from The Affiliated Nanhua Hospital, University of South China. This work was authorized by the ethics committee of The Affiliated Nanhua Hospital of USC (REC reference 2023-KY-233).

1.2. Preparation of ion-selective electrode. The suede was coated with aluminum oxide powder, which had a particle size of 0.05 μm. Then, a small amount of ultra-pure water was added, and the electrode body was polished for 3 min using a suede cloth. Next, it was washed with ultra-pure water. Then, the main body of the electrode was washed using ultrasonic cleaning in a 50.0% ethanol solution for 30 to 60 seconds. It was then immersed in ultra-pure water for an additional 30 to 60 seconds

and subsequently rinsed with ultra-pure water. After drying the electrode, 4 μL of the conductive polymer poly(3-ethylenedioxythiophene) -poly(styrene sulfonic acid) was applied using a liquid transfer gun and coated onto the electrode surface. The coated electrode was then dried for 12 hours.

In order to prepare a creatinine cation-selective electrode membrane, 1 mg of Potassium tetrakis[3,5-bis(trifluoromethyl)phenyl]borate (1 wt%), 3 mg of 2a/2b (3 wt%), 33 mg of PVC (33 wt%), and 66 mg of NOPE (66 wt%) were dissolved in 1 mL of THF. The membranes were vigorously shaken for 30 minutes in an ultrasonicator bath until a complete dissolution of all the components. The solution was then placed in the refrigerator for 4 hours to form a uniform membrane solution. Apply 3 μL of the membrane solution evenly on the electrode at intervals of 3 minutes each time. Repeat this process 5 times and allow it to dry overnight. The electrode membrane was immersed in a 1 mM creatinine and 1 mM KCl solution for 12 hours before being utilized.

1.3. Electrochemical instrumentation and measurements. The previously mentioned creatinine selective electrodes, Ag/AgCl electrode, and platinum sheet electrode were immersed in beakers to measure the responses to creatinine and other interferences. Electromotive force (EMF) response of the creatinine selective electrode was obtained on a Chenhua CHI660E electrochemical workstation.

1.4. Analysis of real samples.

Random urine samples were tested in a 50 mM CH_3COOH-CH_3COONa buffer at pH 3.5. The urine samples were diluted at ratios of 1:10, 1:50 and 1:100 in order to evaluate the influence of different dilution levels on the accuracy of detection results. The results were compared with a standard enzymatic method using the Cobas c702. When the dilution is 1:100, the results closely match the best predictions. Therefore, this dilution factor was selected to detect creatinine in all urine samples (n = 60). For the blood samples, 1:10 dilution was selected considered the concentration range of the blood samples.

2. Synthetic Procedures

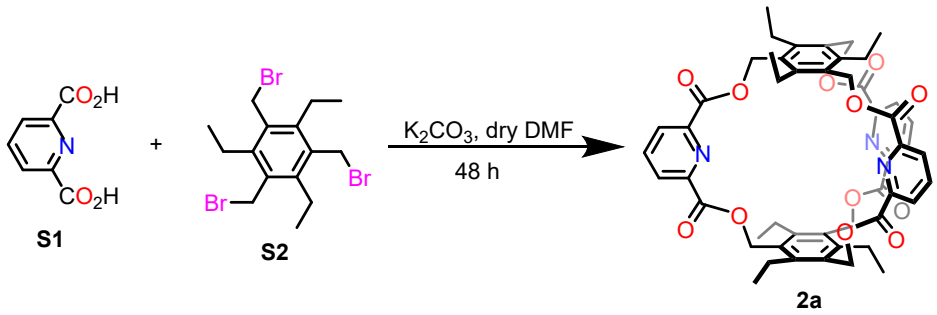

Optimized procedure for the synthesis of 2a: K_2CO_3 (11.1 g, 80.0 mmol) and 500 mL dry DMF were added into a 1000 mL three-neck flask charged with a magnetic stirring bar. The flask was then evacuated and refilled with Ar (using a gas balloon). The solution of **S1** (2.0 g, 12.0 mmol, in 60 mL dry DMF) and **S2** (3.5 g, 8.0 mmol, in 60 mL dry DMF) was added dropwise using two separate syringes to the flask via a double-channel syringe pump during 2 h. Then the reaction mixture was stirred for another 2 h at 80 °C. After removing most of the solvent in vacuum, the residue was poured into ice water (200 mL). The precipitate was then filtered and washed with water extensively to give an off-white solid, which was purified by column chromatography (SiO_2, PE:EA = 10:1~2:1) to afford pure products **2a** (0.83 g, yield 23%). ^{1}H NMR(500 MHz, CD_2Cl_2) δ 8.44 (d, J = 7.9 Hz, 6H), 8.03 (t, J = 7.9 Hz, 3H), 5.44 (s, 12H), 2.78 (q, J = 7.5 Hz, 12H), 1.15 (t, J = 7.5 Hz, 18H). ^{13}C NMR (126 MHz, CD_2Cl_2) δ 166.63, 149.01, 148.48, 138.30, 129.56, 129.53, 63.37, 23.96, 16.55. ESI-HRMS: m/z calcd for $[M+H]^+$ $C_{51}H_{52}N_3O_{12}$, 898.3546; found 898.3561; calcd for $[M+NH_4]^+$ $C_{51}H_{55}N_4O_{12}$, 915.3811; found 915.3826; calcd for $[M+Na]^+$ $C_{51}H_{51}N_3NaO_{12}$, 920.3365; found 920.3379.

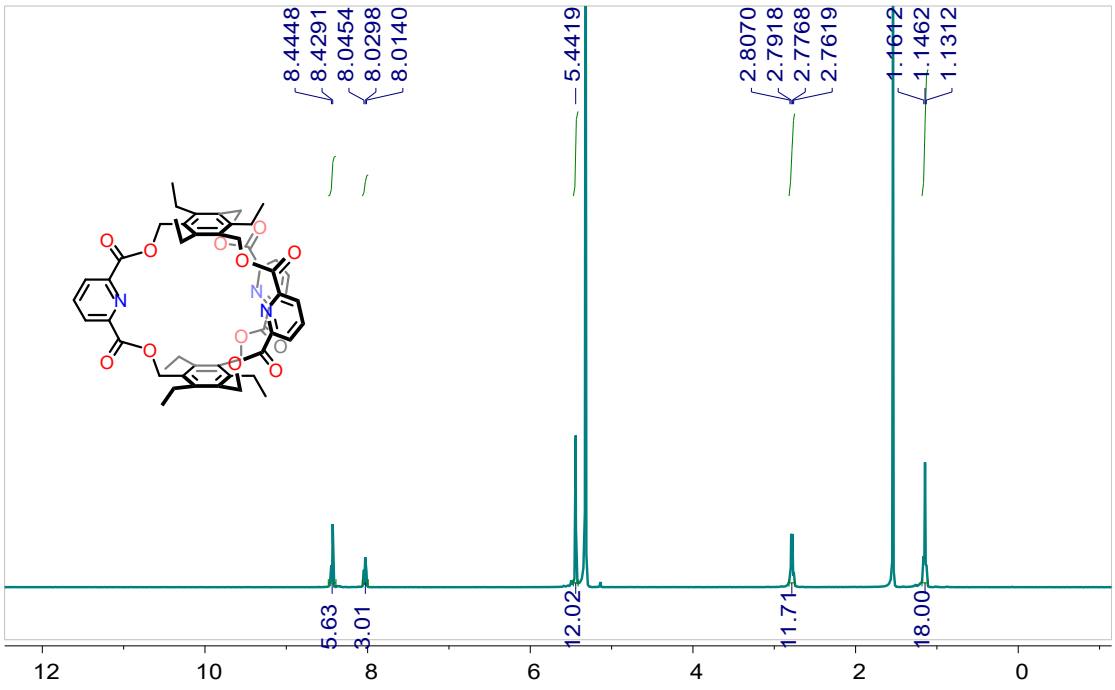

^{1}H NMR spectrum (500 MHz, CD_2Cl_2, 298 K) of **2a**

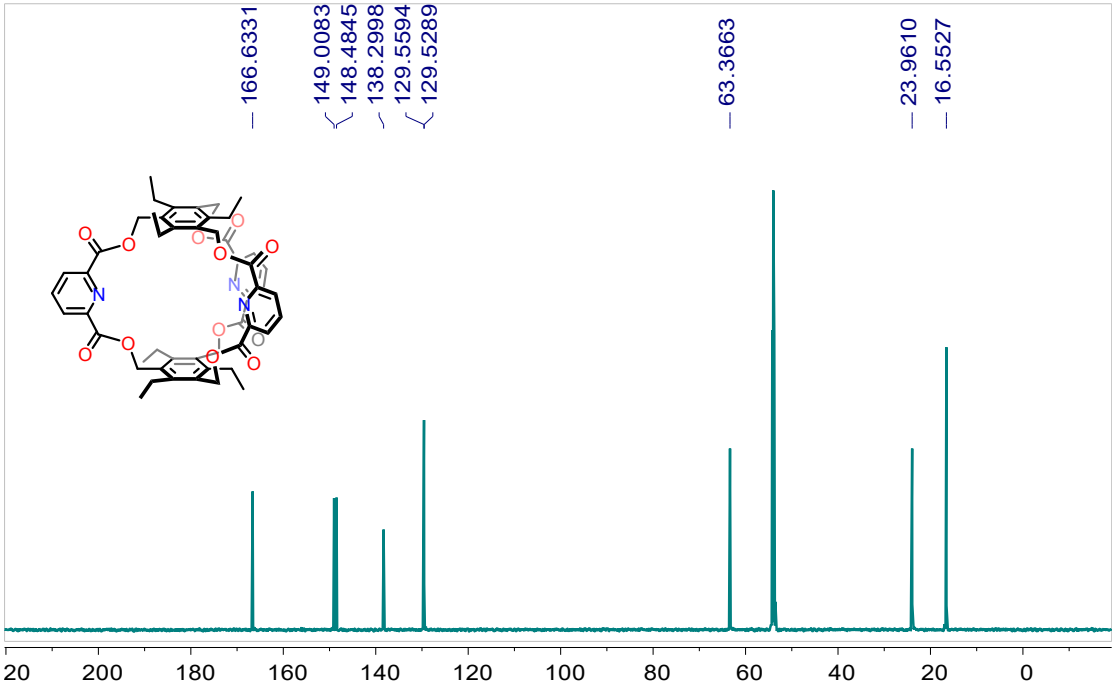

^{13}C NMR spectrum (126 MHz, CD_2Cl_2, 298 K) of **2a**

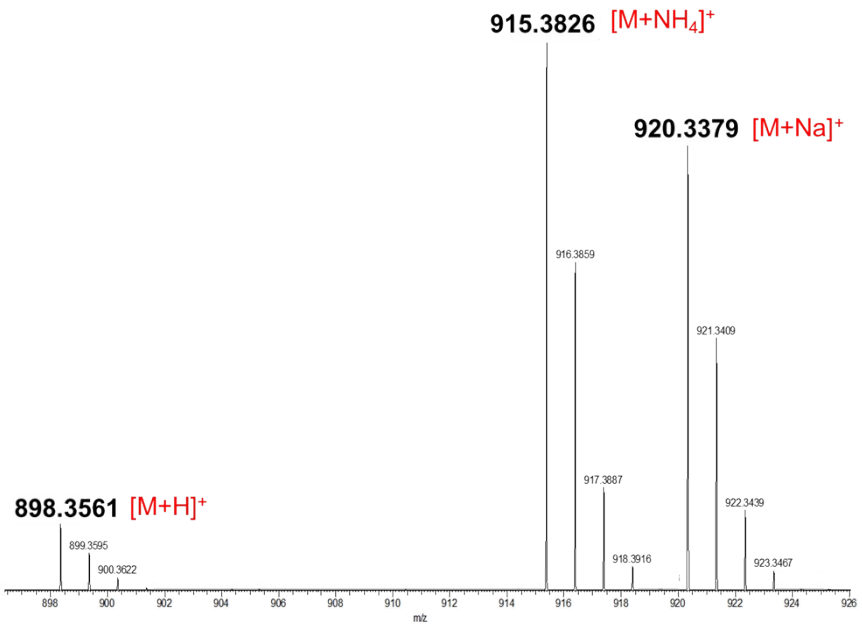

ESI mass spectrum of compound **2a**

Table S1: Synthesis of **2a** in different reaction conditions

Entry	Base	Time	Yield [b]
1 [a]	K_2CO_3	4 h	23%
2 [a]	K_2CO_3	10 h	20%
3 [a]	K_2CO_3	24 h	12%
4 [a]	Cs_2CO_3	4 h	17%
5 [a]	Na_2CO_3	4 h	15%

[a] All reactions were carried out similarly to the optimized procedures described above: with 12.0 mmol **S1**, 8.0 mmol **S2**, and 80.0 mmol base in 500 mL of DMF at 80 °C. [b] Isolated yield.

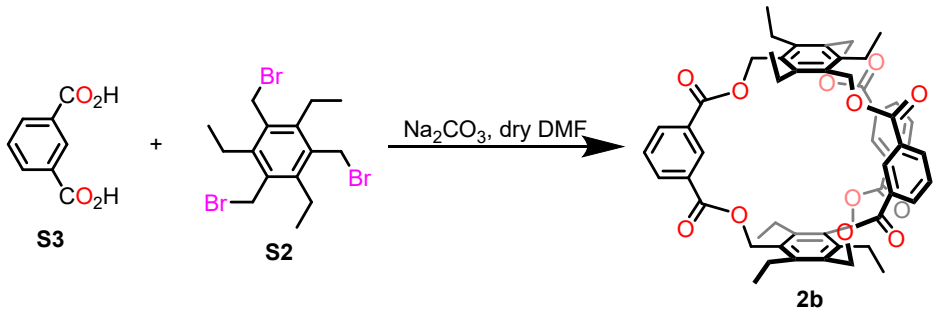

Optimized procedure for the synthesis of 2b: Na_2CO_3 (9.0 g, 80 mmol) and 500 mL dry DMF were added into a 1000 mL three-neck flask charged with a magnetic stirring bar. The flask was then evacuated and refilled with Ar (using a gas balloon). The solution of **S3a** (2.0 g, 12.0 mmol, in 60 mL dry DMF) and **S2a** (3.5 g, 8.0 mmol, in 60 mL dry DMF) was added dropwise using two separate syringes to the flask via a double-channel syringe pump during 10 h. Then the reaction mixture was stirred for another 38 h at 80 °C. After removing most of the solvent in vacuum, the residue was poured into water (200 mL). The precipitate was then filtered and washed with water extensively to give an off-white solid, which was purified by column chromatography (SiO_2, PE : EA = 10:1~5:1) to afford pure products **2b** (1.5 g, yield 42 %). White solid; ^{1}H NMR(500 MHz, CD_2Cl_2) δ 8.43 (d, J = 1.5 Hz, 3H), 8.41 (d, J = 1.3 Hz, 6H), 7.65 (t, J = 7.7 Hz, 3H), 5.41 (s, 12H), 2.76 (q, J = 7.5 Hz, 12H), 1.15 (t, J = 7.5 Hz, 18H). ^{13}C NMR (126 MHz, CD_2Cl_2) δ 166.85, 148.37, 135.71, 130.95, 129.98, 129.43, 128.99, 62.82, 23.75, 16.46. ESI-HRMS : m/z calcd for $[M+Na]^+$ $C_{54}H_{54}NaO_{12}$, 917.3507; found 917.3516.

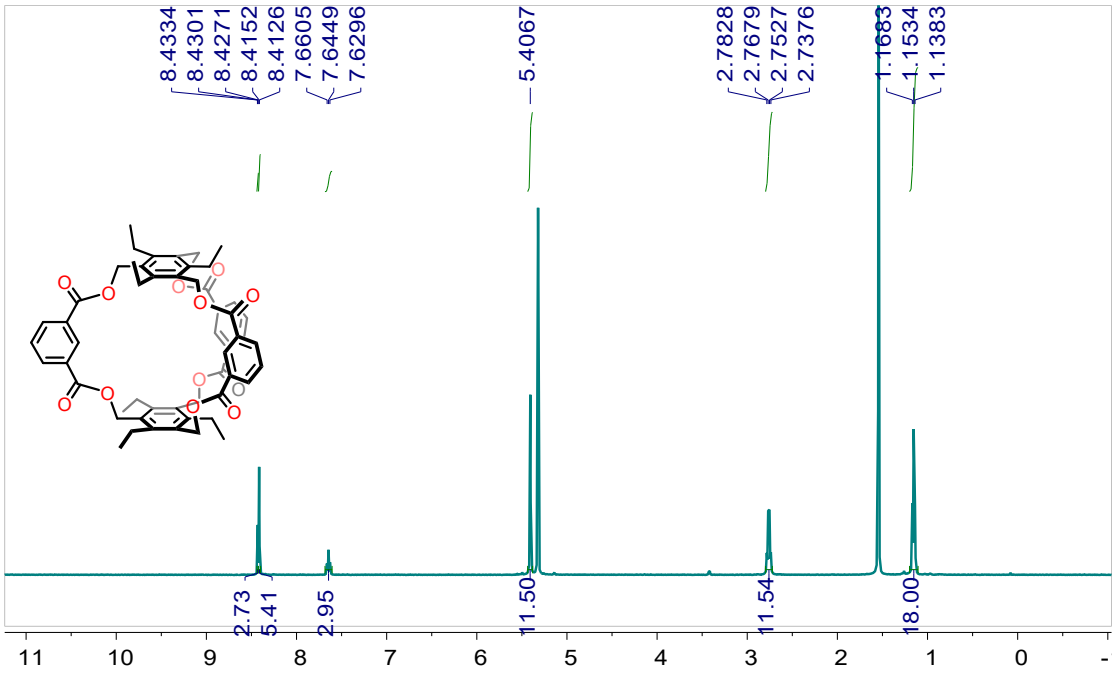

^{1}H NMR spectrum (500 MHz, CD_2Cl_2, 298 K) of **2b**

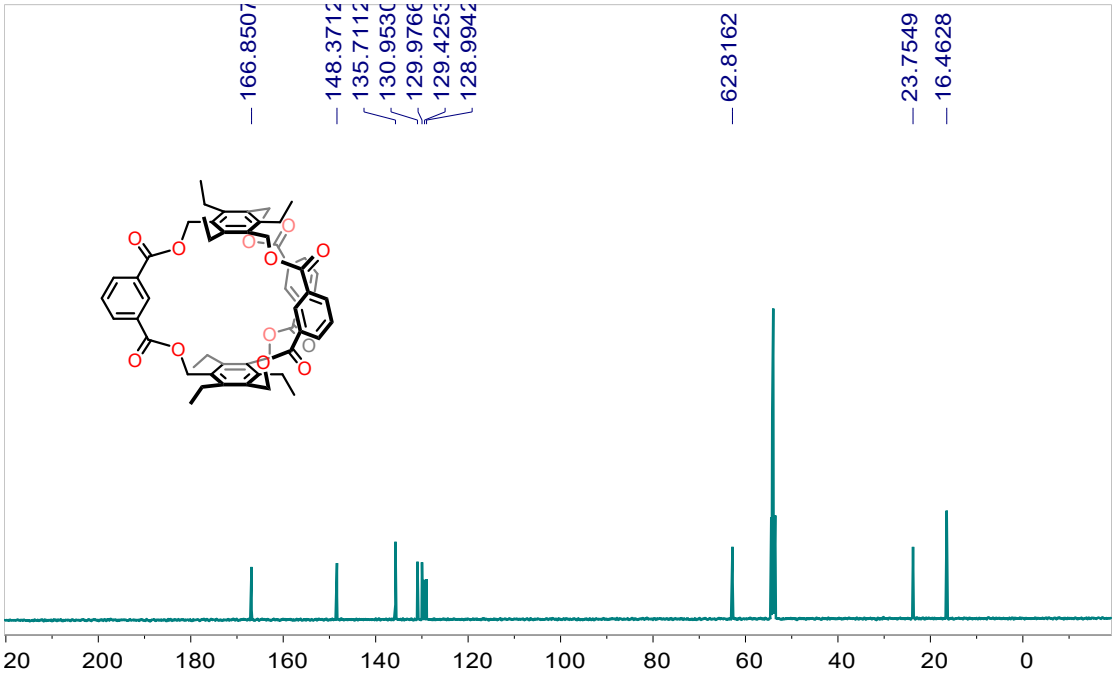

^{13}C NMR spectrum (126 MHz, CD_2Cl_2, 298 K) of **2b**

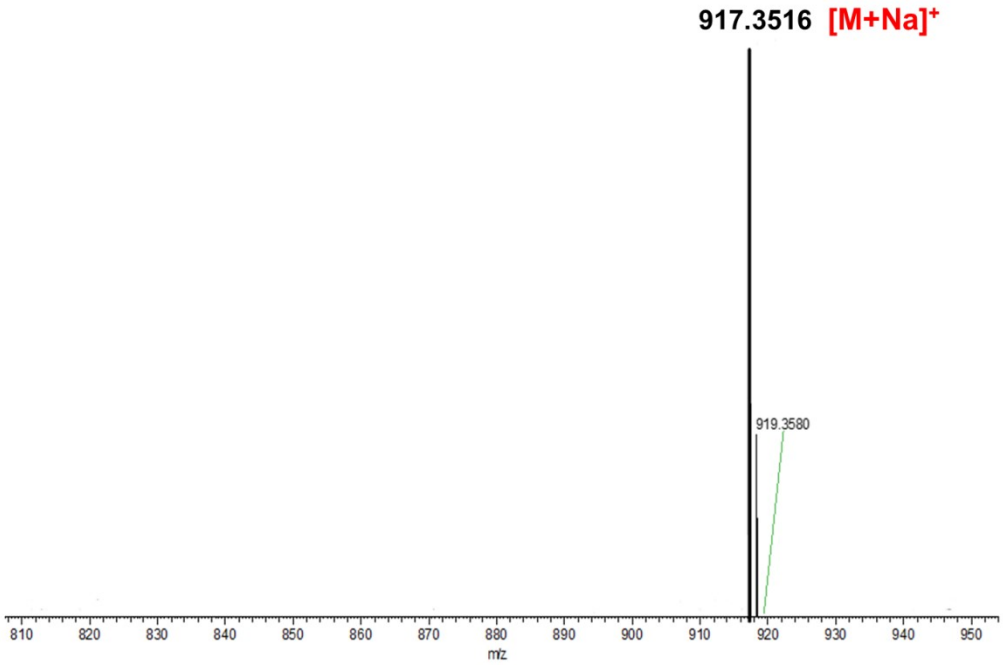

ESI mass spectrum of compound **2b**

Table S2: Synthesis of **2b** in different reaction conditions

Entry	Base	Time	Yield [b]
1 [a]	K_2CO_3	4 h	10%
2 [a]	K_2CO_3	10 h	22%
3 [a]	K_2CO_3	24 h	11%
4 [a]	Cs_2CO_3	10 h	10%
5 [a]	Na_2CO_3	10 h	42%

[a] All reactions were carried out similarly to the optimized procedures described above: with 12.0 mmol **S3**, 8.0 mmol **S2**, and 80.0 mmol base in 500 mL of DMF at 80 °C. [b] Isolated yield.

3. Host-Guest Binding Experiments

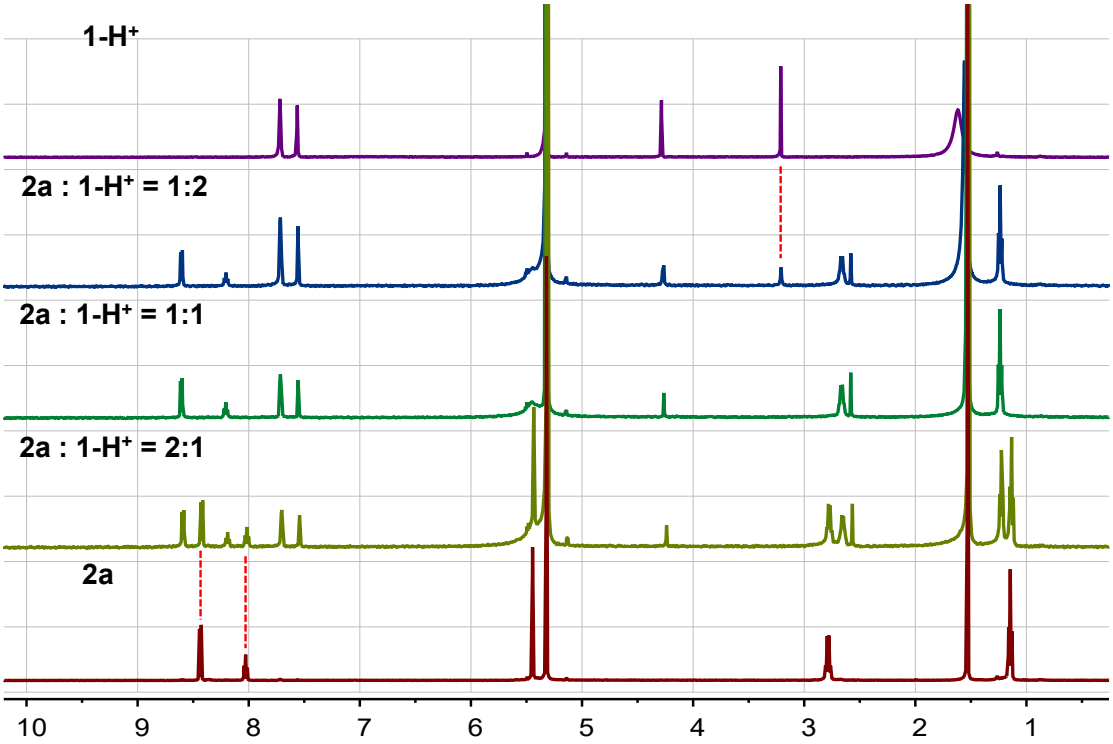

Fig. S1. Full ^{1}H NMR spectra (500 MHz, CD_2Cl_2, 1.0 mM, 298 K) of **1-H**$^+$, **2a**, and their mixture in 1:2, 1:1, and 2:1 ratio. These experiments suggest that the complex between **1-H**$^+$ and **2a** undergoes slow exchange at the current NMR timescale. Thus, the complete disappearance of the free host and free guest in the 1:1 mixture indicates a strong binding between them. We assume that the detection limit of the NMR instrument to be 10%, and use the current concentration 1.0 mM. We may estimate the binding constant to be $(0.90 \times 1.0\ \text{mM})/(0.10 \times 1.0\ \text{mM})^2 = 9.0\times10^4\ \text{M}^{-1}$. Thus, we estimate a lower limit for the binding constant of $9.0\times10^4\ \text{M}^{-1}$.

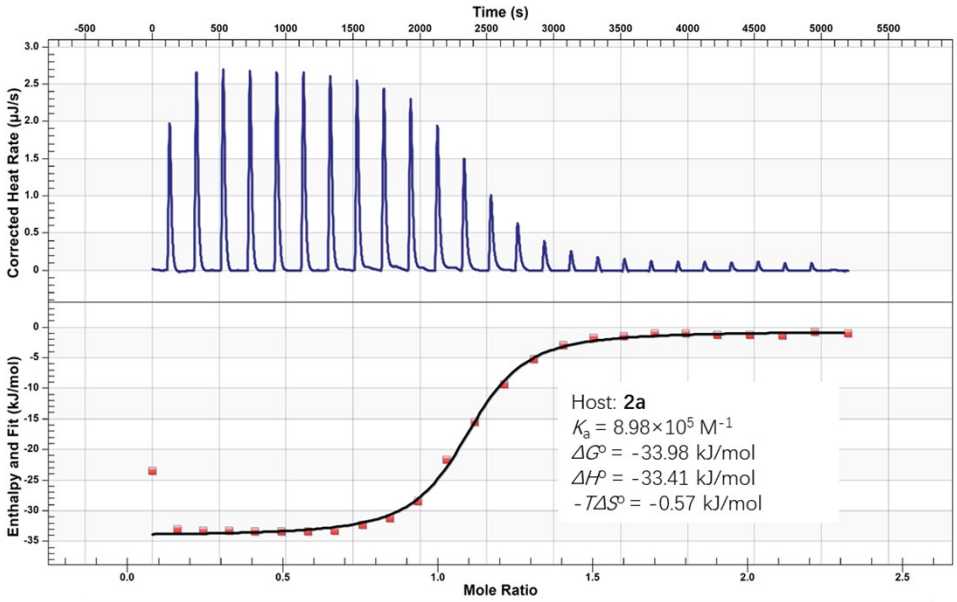

	K_a (M^{-1})	ΔG^o (kJ/mol)	ΔH^o (kJ/mol)	$-T\Delta S^o$ (kJ/mol)
1st	8.98×10^5	-33.98	-33.41	-0.57
2nd	8.26×10^5	-33.77	-32.50	-1.27
3rd	8.59×10^5	-33.87	-32.74	-1.13
average	$(8.61\pm0.36)\times10^5$	-33.87±0.01	-32.88±0.47	0.99±0.37

Fig. S2. Titration plots (heat rate versus time and heat versus guest/host ratio) obtained from ITC experiments of **2a** with **1**-BarF in 1,2-dichloroethane. Dichloroethane was chosen as the experimental solvent primarily due to its higher boiling point than CH_2Cl_2 , making it less volatile compared to dichloromethane.

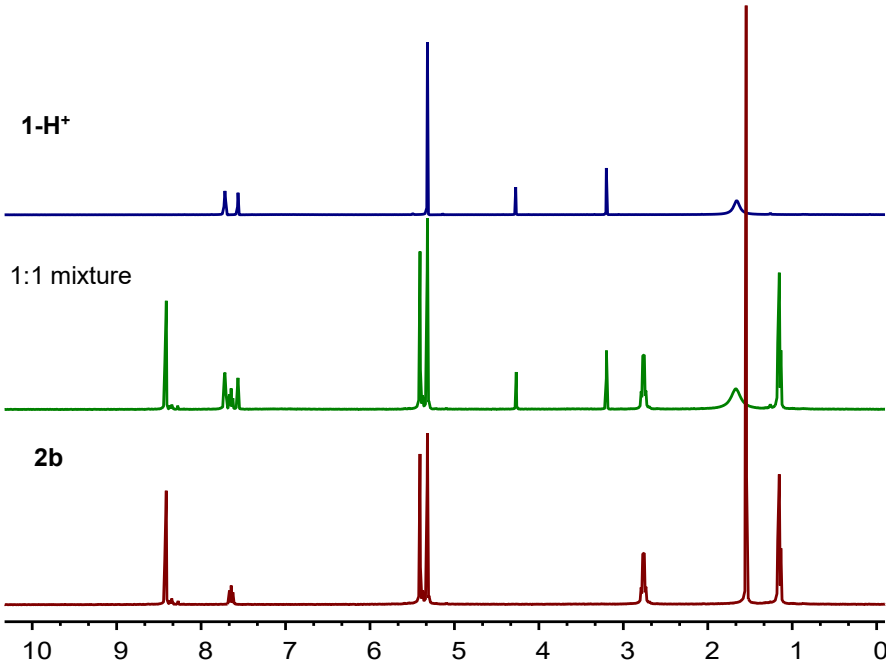

Fig. S3. ^{1}H NMR spectra (500 MHz, CD_2Cl_2, 1.0 mM, 298 K) of **1-H$^+$**, **2b**, and their mixture in 1:1 ratio.

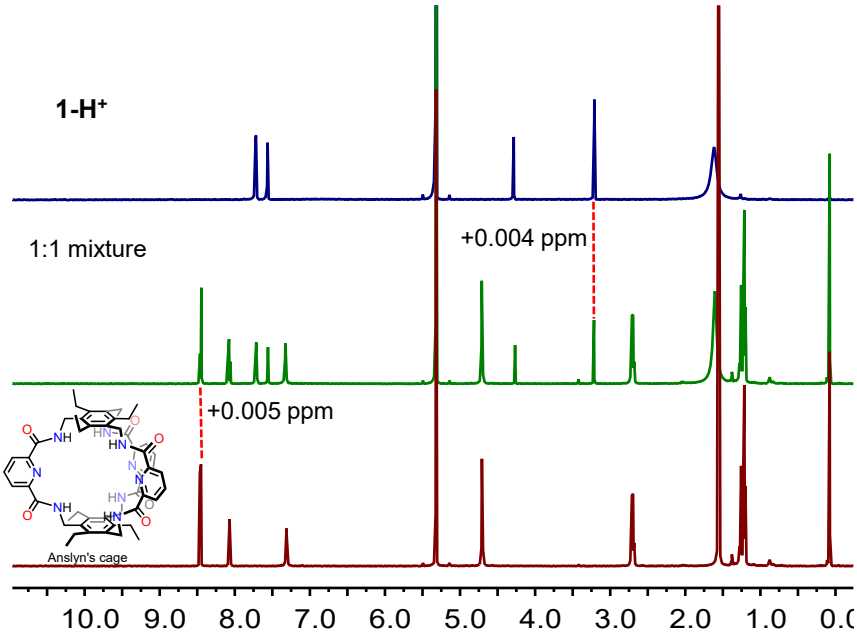

Fig. S4. ^{1}H NMR spectra (500 MHz, CD_2Cl_2, 1.0 mM, 298 K) of **1-H**$^{+}$, Anslyn's cage, and their mixture in 1:1 ratio. The minor shifts in chemical properties observed in the host and guest within the mixture suggest a weak binding interaction between the cavity and the guest.

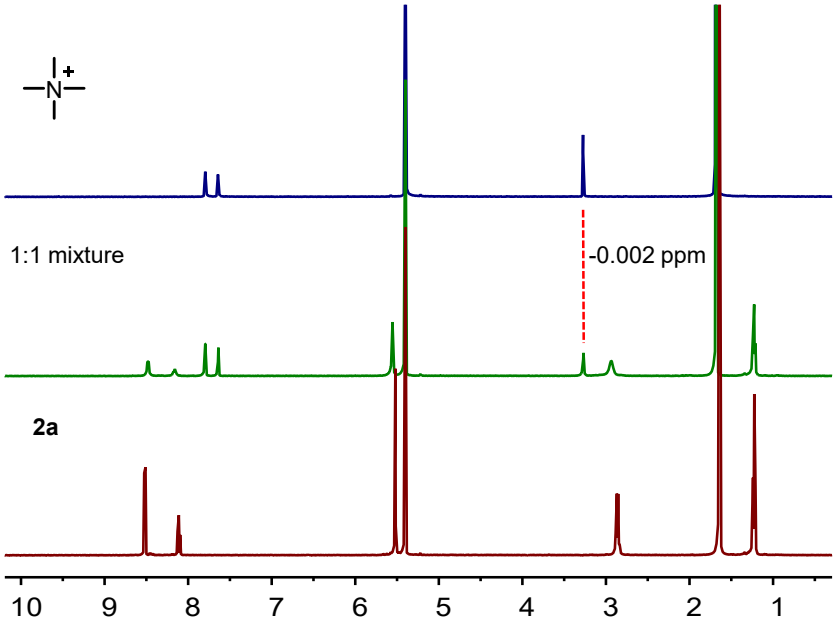

Fig. S5. ^{1}H NMR spectra (500 MHz, CD_2Cl_2, 1.0 mM, 298 K) of tetramethyl ammonium, **2a**, and their mixture in 1:1 ratio. The minor shifts in chemical properties observed in the host and guest within the mixture suggest a weak binding interaction between the cavity and the guest.

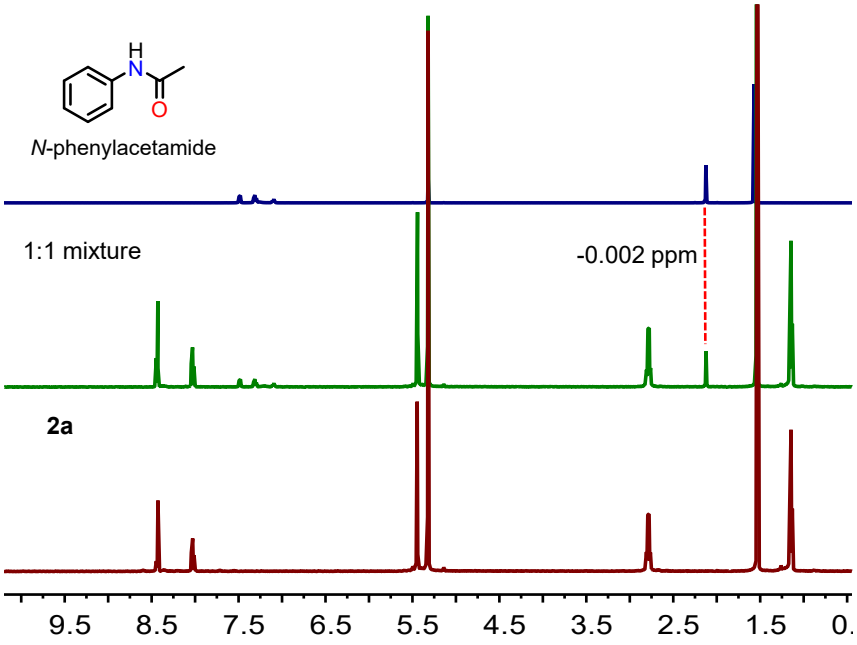

Fig. S6. ^{1}H NMR spectra (500 MHz, CD_2Cl_2, 1.0 mM, 298 K) of *N*-phenylacetamide, **2a**, and their mixture in 1:1 ratio. The minor shifts in chemical properties observed in the host and guest within the mixture suggest a weak binding interaction between the cavity and the guest.

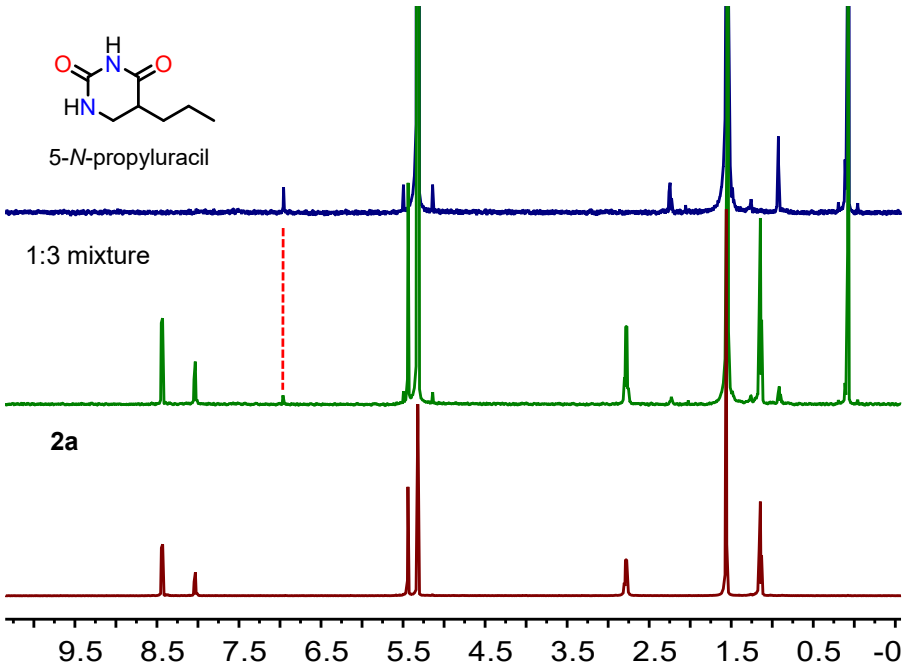

Fig. S7. ^{1}H NMR spectra (500 MHz, CD_2Cl_2, 1.0 mM, 298 K) of 5-*N*-propyluracil, **2a**, and their mixture in 1:3 ratio. The minor shifts in chemical properties observed in the host and guest within the mixture suggest a weak binding interaction between the cavity and the guest.

4. Computational data

Quantum chemistry calculations were performed by using Gaussian 16 package.[1] The structure of the complexes between host and guest has been optimized employing density functional theory (DFT) with dispersion corrected method (wB97XD)[2] in combination with 6-31G* basis set (the Polarizable Continuum Model (PCM) water model was used).[3] Independent gradient model (IGMH) analysis[4] were carried out with Multiwfn 3.8 (dev) program.[5] Molecular plots were visualized by the VMD 1.9.3 program.[6] Electrostatic potential of the vdW surface was carried out with Multiwfn 3.8 (dev) program and visualized by the VMD 1.9.3 program. The volumes of the guest and the cavity of hosts were calculated by MoloVol[7] (single-probe mode for volume of guest: small probe radius: 1.2 Å, grid resolution: 0.1; two-probe mode for volume of the cavity of host: small probe radius: 1.2 Å, large probe radius: 6 Å, grid resolution: 0.1).

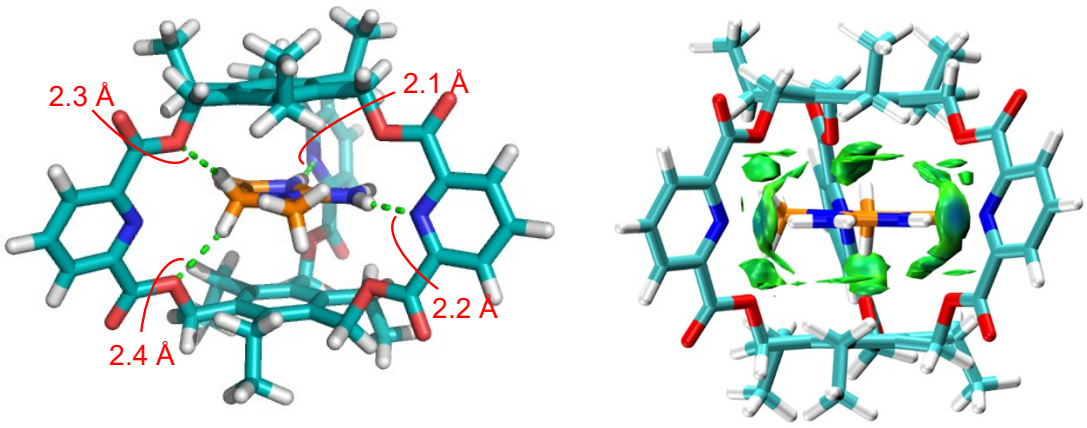

Fig. S8. Energy-minimized structures and visual analysis of intermolecular interactions (IGMH) of **1-H$^+$@2a** in water obtained by DFT (wB97XD/6-31G(d)) calculations. The dotted lines indicate the hydrogen bonds.

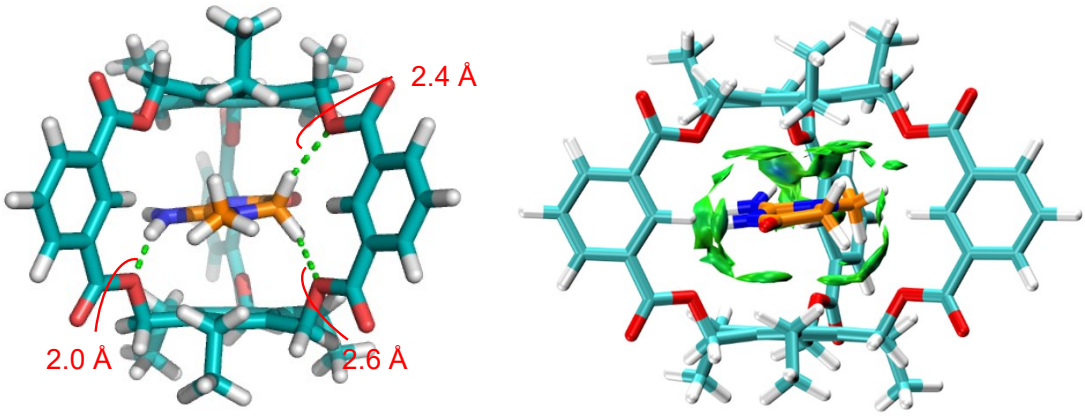

Fig. S9. Energy-minimized structures and visual analysis of intermolecular interactions (IGMH) of **1-H$^+$@2b** in vacuum obtained by DFT (wB97XD/6-31G(d)) calculations. The dotted lines indicate the hydrogen bonds.

Table S3. Cavity volumes of host (Å^3), guest volume (Å^3), and derived packing coefficient for the complex.

complexes	cavity volume	guest volume	packing coefficient
1-H$^+$@2a	166.5	110.9	67%
1-H$^+$@2b	161.9	110.9	69%

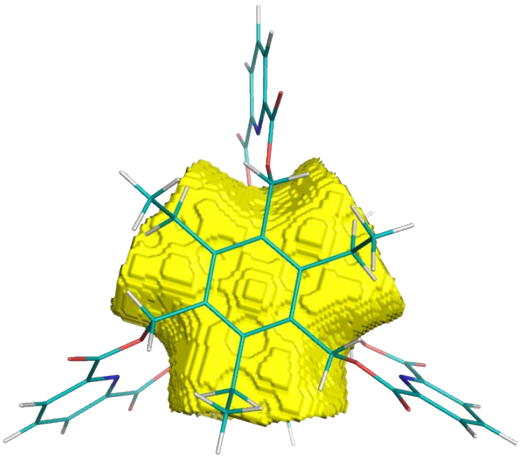

Fig. S10 The volume of the cavity of **2a** was calculated to be 166.5 Å^3 by MoloVol (Enable two-probe mode: small probe radius: 1.2 Å, large probe radius: 6 Å, grid resolution: 0.1).

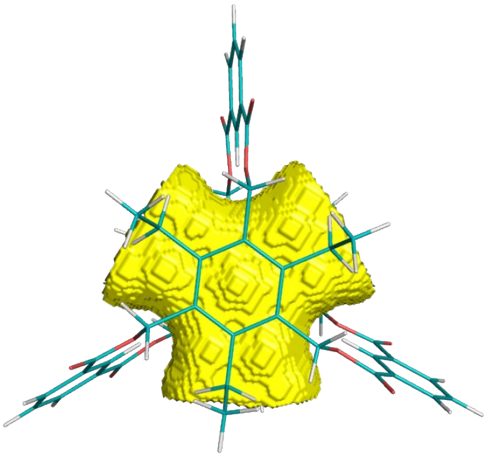

Fig. S11 The volume of the cavity of **2b** was calculated to be 161.9 $Å^3$ by MoloVol (small probe radius: 1.2 Å, large probe radius: 6 Å, grid resolution: 0.1).

5. Electrochemical experiment

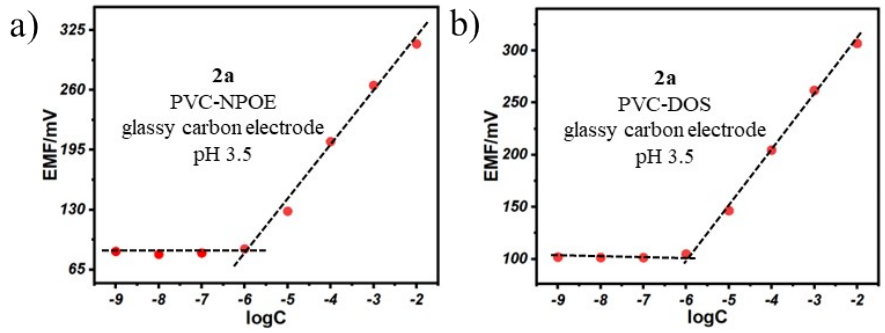

plasticizer	LOD (M)	Slope (mV/dec^{-1})	Linear range	R^2
DOS	-6.00	51.95	10^{-6}-10^{-2}	0.998
NPOE	-6.02	58.19	10^{-6}-10^{-2}	0.995

Fig. S13. Calibration curves of EMF responses to different concentrations of creatininium for electrodes containing **2a** as the ionophore and various membrane plasticizers.

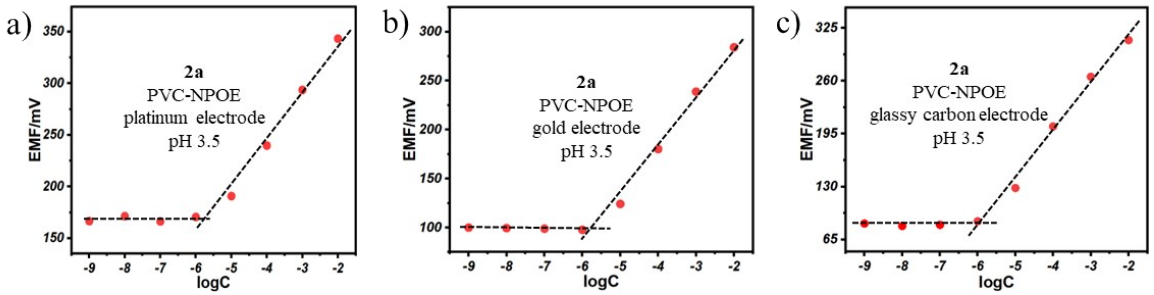

Conductive medium	LOD (M)	Slope (mV/dec^{-1})	Linear range	R^2
platinum electrode	-5.78	44.8	10^{-6}-10^{-2}	0.990
gold electrode	-5.78	48.76	10^{-6}-10^{-2}	0.993
glassy electrode	-6.02	58.19	10^{-6}-10^{-2}	0.995

Fig. S14. Calibration curves of EMF responses to different concentrations of creatininium for electrodes containing **2a** as the ionophore and various electrodes.

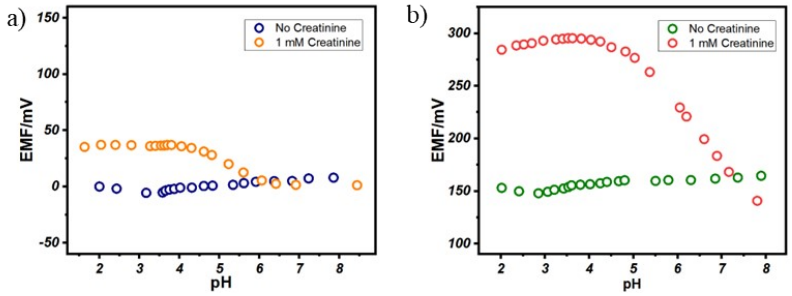

Fig. S15. Potentiometric response upon changes of pH for a (a) blank sensor and (b) **2a**-based electrode in a universal buffer with and without creatinine.

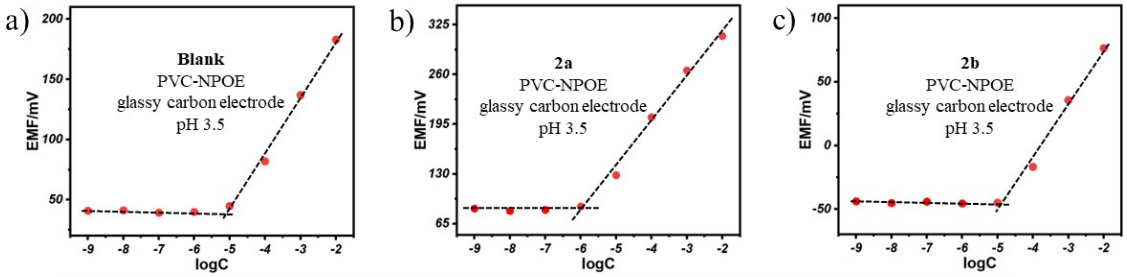

Ionophore	LOD (M)	Slope (mV/dec^{-1})	Linear range	R^2
Blank	-4.99 ± 0.12	39.86 ± 1.16	10^{-5}-10^{-2}	0.997
2a	-6.02 ± 0.07	58.19 ± 0.37	10^{-6}-10^{-2}	0.995
2b	-4.88 ± 0.16	44.81 ± 0.12	10^{-5}-10^{-2}	0.994

Fig. S16. Calibration curves of EMF responses to different concentrations of creatininium cation for electrode without ionophore (a), **2a**-based electrode (b), and **2b**-based electrode (c).

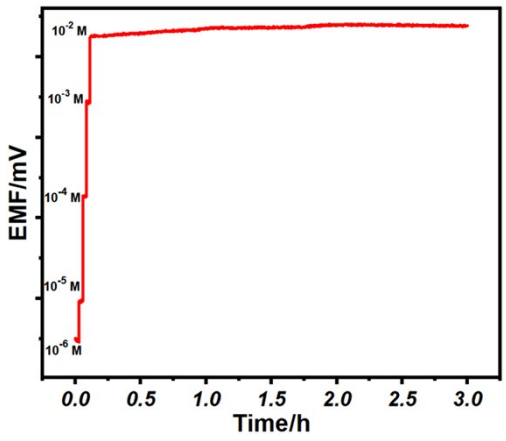

Fig. S17. Stability of **2a**-based electrode running for 3h under 10 mM of creatininium cation in a CH_3COOH-CH_3COONa buffer (pH = 3.5).

Table. S4. The selectivity coefficients for Creatine, K^+, Na^+, NH_4^+, Ca^{2+}, and Urea of the electrodes containing **2a**.

Analytes (j)	Sensor ($\log K_{Cr,j}$)	Analytes (j)	Sensor ($\log K_{Cr,j}$)
Creatine	-4.0 ± 0.01	NH_4^+	-3.8 ± 0.01
K^+	-4.2 ± 0.01	Ca^{2+}	-4.9 ± 0.01
Na^+	-4.7 ± 0.01	Urea	-4.9 ± 0.01

The selectivity coefficients were calculated using equation 1:

$$-\log K_{ij,max}^{Pot} = \frac{E_i - E_j}{S} \quad \text{(eq. 1)}$$

where $K_{ij,max}^{Pot}$ is the highest tolerable value of the selectivity factor, E_i represents the EMF of the ion to be tested, E_j represents the EMF of interfering ions, and S stands for sensitivity.

Table. S5. Comparison of selectivity coefficients obtained with our sensor, and other reported potentiometric sensors.

Analytes (j)	Sensor ($\log K_{Cr,j}$)	Guinovart et al., 2017
K^+	-4.2	-2.5
Na^+	-4.7	-3.7
NH_4^+	-3.8	-2.3
Ca^{2+}	-4.9	-4.8

Table. S6. The ionophore complex formation constant for Creatinine, K^+, Na^+, and NH_4^+ of the electrodes containing **2a**.

Ion I^+	Membrane potential △EMF(mV)	Formation constant Log β_{IL}
Creatinine	301.93 ± 5.92	6.69 ± 0.10
K+	126.73 ± 1.64	3.73 ± 0.02
Na+	109.36 ± 0.41	3.43 ± 0.01
NH_4^+	157.00 ± 0.40	4.24 ± 0.01

The ionophore complex formation constant were calculated using the following

equation:

$$\beta_{IL} = (L_T - \frac{nR_T}{z_I})^{-n} exp(\frac{E_M z_I F}{RT}) \quad \text{(eq. 2)}$$

where L_T is the total concentration of ionophore in the membrane segment, n is the stoichiometry, R_T is the concentration of lipophilic ionic sites and E_M is the potential for a two-segment membrane. For the calculation of the binding constants, we assumed throughout this work that the stoichiometry is n=1.

6. X-Ray Single Crystallography

Suitable single crystals of **2a** and **2b** were successfully obtained by slow liquid diffusion of hexane into a solution of CH_2Cl_2. Single crystal X-ray data were collected on a Bruker D8 VENTURE with Ga Kα radiation (λ = 1.34138 Å) at 100 K. The structures were solved by intrinsic phasing methods (SHELXT[8]) and refined by full-matrix least squares on F^2 using SHELXL in the OLEX2 program package. All non-hydrogen atoms were refined with anisotropic thermal parameters and the hydrogen atoms were fixed at calculated positions and refined by a riding mode. SQUEEZE[9] routine implemented on PLATON was used to remove electron densities corresponding to disordered solvent molecules in the crystal data.

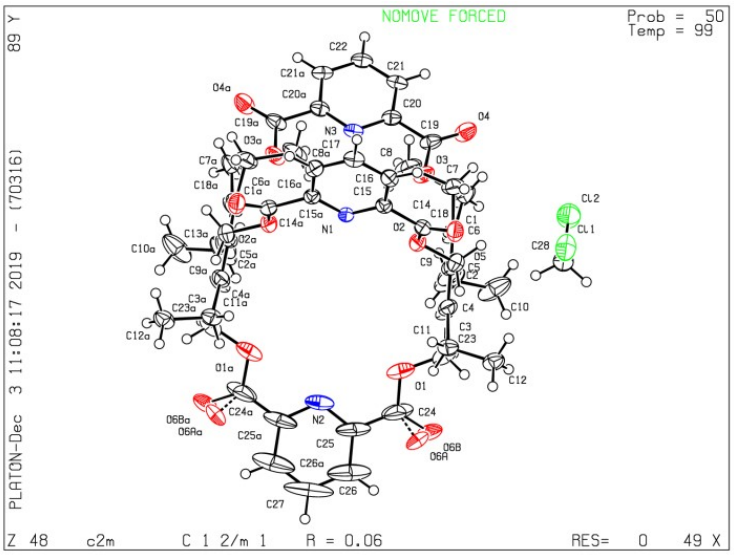

Crystal structure of **2a**·CH_2Cl_2

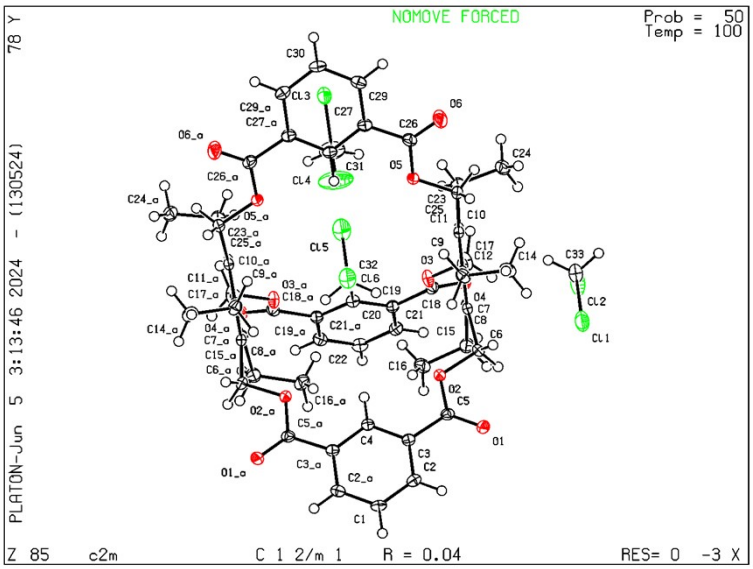

Crystal structure of **2b**·$3CH_2Cl_2$

Table *S7.* Crystal data and structure refinement for hosts **2a** and **2b**

entry	**2a**•CH_2Cl_2	**2b**•$3CH_2Cl_2$
Moiety formula	$0.5(C_2H_4Cl_4)\cdot C_{51}H_{51}N_3O_{12}$	$1.5(C_2H_4Cl_4)\cdot C_{54}H_{54}O_{12}$
Empirical formula	$C_{52}H_{53}O_{12}N_3Cl_2$	$C_{57}H_{60}Cl_6O_{12}$
Formula weight	982.87	1149.75
Temperature/K	99.23	100.0
Crystal system	monoclinic	monoclinic
Space group	*C*2/*m*	*C*2/*m*
a/Å	22.6288(6)	22.161 (2)
b/Å	14.0186(4)	14.1881 (13)
c/Å	17.8883(5)	17.9966 (17)
α/°	90	90
β/°	104.328(10)	102.595 (3)
γ/°	90	90
Volume/Å^3	5498.1(3)	5522.4 (9)
Z	4	4
ρ_{calc}g/cm^3	1.187	1.383
μ/mm^{-1}	1.554	2.215
F(000)	2064.0	2400.0
Reflections collected	15554	35409
Independent reflections	4143 [R_{int} = 0.0373, R_{sigma} = 0.0335]	5888 [R_{int} = 0.0691, R_{sigma} = 0.0544]
Data/restraints/parameters	4143/0/338	5888/0/364
Goodness-of-fit on F^2	1.082	1.061
Final R indexes [I>=2σ (I)]	R_1 = 0.0613, wR_2 = 0.1531	R_1 = 0.0426, wR_2 = 0.1160
Final R indexes [all data]	R_1 = 0.0735, wR_2 = 0.1615	R_1 = 0.0478, wR_2 = 0.1204
CCDC number	2323488	2360598

7. Reference

[1] Gaussian 16, Revision B.01, M. J. Frisch, G. W. Trucks, H. B. Schlegel, G. E. Scuseria, M. A. Robb, J. R. Cheeseman, G. Scalmani, V. Barone, G. A. Petersson, H. Nakatsuji, X. Li, M. Caricato, A. V. Marenich, J. Bloino, B. G. Janesko, R. Gomperts, B. Mennucci, H. P. Hratchian, J. V. Ortiz, A. F. Izmaylov, J. L. Sonnenberg, D. Williams-Young, F. Ding, F. Lipparini, F. Egidi, J. Goings, B. Peng, A. Petrone, T. Henderson, D. Ranasinghe, V. G. Zakrzewski, J. Gao, N. Rega, G. Zheng, W. Liang, M. Hada, M. Ehara, K. Toyota, R. Fukuda, J. Hasegawa, M. Ishida, T. Nakajima, Y. Honda, O. Kitao, H. Nakai, T. Vreven, K. Throssell, J. A. Montgomery, Jr., J. E. Peralta, F. Ogliaro, M. J. Bearpark, J. J. Heyd, E. N. Brothers, K. N. Kudin, V. N. Staroverov, T. A. Keith, R. Kobayashi, J. Normand, K. Raghavachari, A. P. Rendell, J. C. Burant, S. S. Iyengar, J. Tomasi, M. Cossi, J. M. Millam, M. Klene, C. Adamo, R. Cammi, J. W. Ochterski, R. L. Martin, K. Morokuma, O. Farkas, J. B. Foresman, and D. J. Fox, Gaussian, Inc., Wallingford CT, **2016**.

[2] Chai, J.-D.; Head-Gordon, M. *Phys. Chem. Chem. Phys.* **2008**, *10*, 6615-6620.

[3] (a) Cances, E.; Mennucci, B.; Tomasi, J. *J. Chem. Phys.* **1997**, *107*, 3032; (b) Mennucci, B.; Tomasi, J. *J. Chem. Phys.* **1997,** *106*, 5151.

[4] Lefebvre, C.; Rubez, G.; Khartabil, H.; Boisson, J.-C.; Contreras-García, J.; Hénon, E. *Phys. Chem. Chem. Phys.* **2017**, *19*, 17928-17936.

[5] Lu, T.; Chen, F. *J. Comput. Chem.* **2012**, *33*, 580-592.

[6] Humphrey, W.; Dalke, A.; Schulten, K. *J. Mol. Graph. Model.* **1996**, *14*, 33-38.

[7] Maglica, J. B.; Lavendomme, R. *J. Appl. Crystallogr.* **2022**, *55*, 1033-1044..

[8] Sheldrick, G. M. *Acta Cryst.* **2015**, *A71*, 3-8.

[9] Spek, A.L. *Acta Cryst.* **2009**, *D65*, 148-155.